

# Photochemical Reactions of Nitroso Oxides at Low Temperatures: The First Experimental Evidence for Dioxaziridines

T. Harder, P. Wessig, J. Bendig,\* and R. Stösser

Contribution from the Institute of Chemistry, Humboldt University Berlin, Hessesche Strasse 1-2, 10115 Berlin, Germany

Received February 2, 1998. Revised Manuscript Received March 25, 1999

**Abstract:** Several singlet nitroso oxides (**3a–e**) were generated by the thermal reaction of triplet nitrenes (**2a–e**) with triplet oxygen at 95 K in 2-methyltetrahydrofuran. After photolysis of the nitroso oxides at 77 K using strong light intensities, the formation of intermediates was observed for the first time. From spectroscopic, kinetic, and chemical arguments, we postulate the formation of the following dioxaziridines: 4-(dioxaziridin-yl)stilbene (**4a**), 4-(dioxaziridin-yl)-4'-nitrostilbene (**4b**), 4'-(dioxaziridin-yl)-4-(dimethylamino)stilbene (**4c**), 4'-(dioxaziridin-yl)-4-aminobiphenyl (**4d**), and 4-(dioxaziridin-yl)-4'-(nitrene-substituted)stilbene (**4f**). All dioxaziridines observed are highly reactive species. At 77 K, they react thermally to form the corresponding nitro compounds (**5**). The velocity of the ring opening reaction of the dioxaziridines (**4** → **5**) is not significantly influenced by substituents; the rate constants at 77 K are all equal to  $0.0030 \pm 0.0005 \text{ s}^{-1}$ . The transients were characterized by stationary UV/vis and/or ESR spectroscopy. Ab initio calculations of the thermal reaction of the nonsubstituted dioxaziridine (**6**) and *N*-phenyldioxaziridine (**9**) were performed. From this, it follows that dioxaziridines are experimentally observable species which are separated from the corresponding nitro products by an orbital symmetry-forbidden barrier.

## Introduction

Organic chemists have been interested in the properties of ROO species such as carbonyl oxides, dioxiranes, nitroso oxides, and dioxaziridines for years.<sup>1–3</sup> While a large amount of experimental and theoretical information about the carbon species is available, little is known about the analogous nitrogen intermediates. Trapping experiments indicate that nitroso oxides are formed by the reaction of *p*-nitrophenylnitrene and oxygen at room temperature.<sup>2</sup> Furthermore nitroso oxides were detected at low temperatures (77–120 K). They are spectroscopically characterized by broad long-wavelength UV/vis absorption bands.<sup>4,5</sup>

Only little information is available about the reactions of nitroso oxides. After excitation of nitroso oxides at 77 K, the exclusive formation of the corresponding nitro compounds was found by product analysis and by spectroscopic results.<sup>4,5</sup> In contrast to the photochemical reaction at 77 K, the thermal reaction of nitroso oxides (**3**) at room temperature is reported to result in the formation of both the corresponding nitro (**5**) and the nitroso compound. It is assumed that the nitro compound is formed via a dioxaziridine intermediate.<sup>2</sup> But the existence of dioxaziridines could not be confirmed so far by direct spectroscopic observations.

From theoretical investigations, it follows that the activation barrier of the conversion of nitroso oxides into dioxaziridines

amounts to about 45 kcal/mol.<sup>6</sup> It is therefore assumed that a possible intramolecular conversion of nitroso oxides into nitro compounds via dioxaziridines has to be initialized photochemically.

In this paper, we report on the generation of nitroso oxides at low temperatures, on their UV/vis and ESR spectroscopic properties, and on their photochemical reactions. Analyzing the photochemical reactions of nitroso oxides in detail, we found the first experimental evidence for the existence of dioxaziridines. On the basis of their UV/vis spectra, we present the kinetics of the thermal reactions of the dioxaziridines **4a–d** and **4f**. Furthermore, we present our results of ab initio calculations (obtained using model compounds) of the thermal reactions of dioxaziridines. They include molecular structures and geometrical parameters of the involved states, their thermodynamic properties, and the stereoelectronic course of the ring opening of dioxaziridines.

The experiments were carried out under conditions which allow separation of all photochemical and thermal processes from each other. This was realized by photolyzing exclusively azides, which form at 77 K only the corresponding triplet nitrenes (without subsequent thermal and photochemical reactions). This is the most important precondition for the success of our experiments, but this condition is not met in the case of phenylnitrene derivatives. On the other hand, the large molecules used in our experiments cannot be treated by quantum chemical calculations at a high level of theory. Qualitative results were therefore obtained by theoretical investigations of C<sub>6</sub> derivatives.

## Synthesis

The azides **1a–e** were synthesized as shown in Figure 1. At first, the corresponding nitro compounds were synthesized by the reaction of 4-(nitrophenyl)acetic acid with the corresponding

(1) Sawaki, Y.; Ishikawa, S.; Iwamura, H. *J. Am. Chem. Soc.* **1987**, *109*, 584.

(2) Ishikawa, S.; Nojima, T.; Sawaki, Y. *J. Chem. Soc., Perkin Trans. 2* **1996**, 127.

(3) Casal, H. L.; Sugamori, S. E.; Scaiano, J. C. *J. Am. Chem. Soc.* **1984**, *106*, 7623. (b) Scaiano, J. C.; McGimpsey, W. G.; Casal, H. L. *J. Org. Chem.* **1989**, *54*, 1612. (c) Sander, W. *J. Org. Chem.* **1989**, *54*, 333. (d) Chapman, O. L.; Hess, T. C. *J. Am. Chem. Soc.* **1984**, *106*, 1842. (e) Liang, T.-Y.; Schuster, G. B. *J. Am. Chem. Soc.* **1987**, *109*, 7803.

(4) Brinen, J. S.; Singh, B. *J. Am. Chem. Soc.* **1971**, *93*, 6623.

(5) Harder, T.; Bendig, J.; Scholz, G.; Stösser, R. *J. Inf. Rec. Mater.* **1996**, *23*, 147.

(6) Fueno, T.; Yokoyama, K.; Takanc, S. *Theor. Chim. Acta* **1992**, *82*, 299.

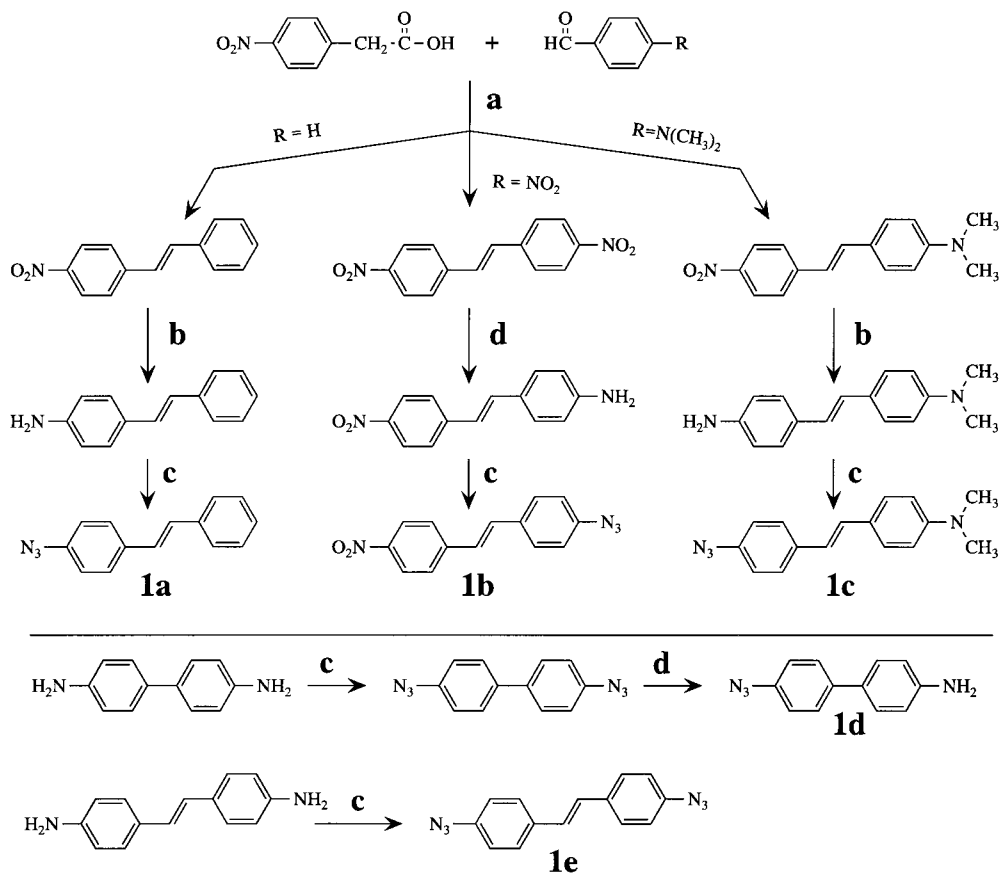


**Figure 1.** Synthesis of the azides and their precursors: (a) piperidine as a catalyst, 140 °C, 2 h; (b) 80% aqueous ethanol, FeSO<sub>4</sub>/NH<sub>3</sub>, 100 °C, 2 h; (c) aqueous HCl/NaNO<sub>2</sub>, 0 °C, NaN<sub>3</sub>; and (d) 85% aqueous ethanol, NaHS, 70 °C.

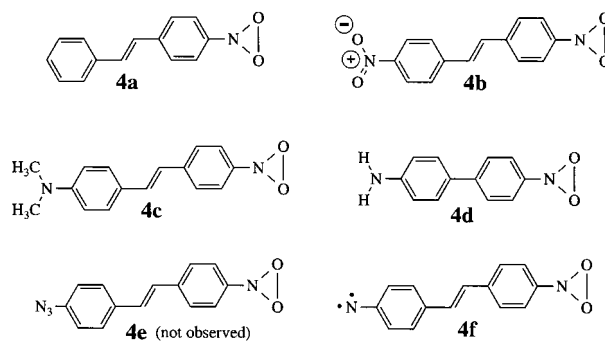
4-substituted benzaldehyde using piperidine as a catalyst ( $T \approx 140$  °C). Alternatively, 4,4'-dinitrostilbene can also be synthesized by the treatment of 4-nitrobenzyl chloride with KOH. The synthesis of 4-aminostilbene and 4-amino-4'-(dimethylamino)-stilbene was realized by a reduction of the corresponding nitro compounds using FeSO<sub>4</sub>/NH<sub>3</sub>. The 4-amino-4'-nitrostilbene was synthesized by a partial reduction of 4,4'-dinitrostilbene using sodium sulfide which was saturated with hydrogen sulfide before. Azides **1a–c**, diazide **1e**, and 4,4'-diazidobiphenyl were synthesized by the diazotation of the corresponding amines or diamines (4,4'-diaminostilbene and 4,4'-diaminobiphenyl were obtained from Aldrich Chemical Co.) and by further treatment with sodium azide at 0 °C. Azide **1d** was obtained by a partial reduction of 4,4'-diazidobiphenyl using sodium sulfide which was saturated with hydrogen sulfide before. All syntheses were carried out under yellow light; the azides were stored in a refrigerator at 5 °C in aluminum foil-wrapped vials.

## Results and Discussion

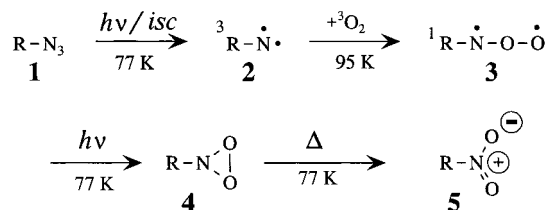
**Photochemistry and Spectroscopy.** The investigated reaction cascade involving all photochemical and thermal steps and including the pathway for generating **4a–d** is illustrated in Scheme 2. The specific procedure for synthesizing species **4f** is shown in Scheme 3.

The triplet nitrenes **2a–d** were formed after the photochemical excitation of the corresponding azides **1a–d** at 77 K in MTHF.<sup>5,7</sup> The samples containing the nitrenes were then immediately warmed to 95 K by a temperature jump (5 K/min). In this way, only nitroso oxides **3a–d** but no amines were

### Scheme 1



### Scheme 2



formed.<sup>8</sup> As an example, these reaction steps are illustrated in Figure 2 using the UV/vis spectroscopic investigations of the reactions of 4-azidostilbene (**1a**). These are as follows. The excitation of **1a** ( $\lambda_{\max} = 319, 333,$  and  $350$  nm) at 77 K in MTHF leads to the quantitative formation of the corresponding 4-nitrene-substituted stilbene (**2a**,  $\lambda_{\max} = 369, 378, 614,$  and  $687$  nm, Figure 2a; ESR:  $|D/hc| = 0.8$  cm<sup>-1</sup>). The linear ED curves indicate that the nitrene **2a** is formed in one observable reaction step and furthermore that **2a** is photochemically and

(7) Harder, T.; Bendig, J.; Scholz, G.; Stösser, R. *J. Am. Chem. Soc.* **1996**, *118*, 2497.

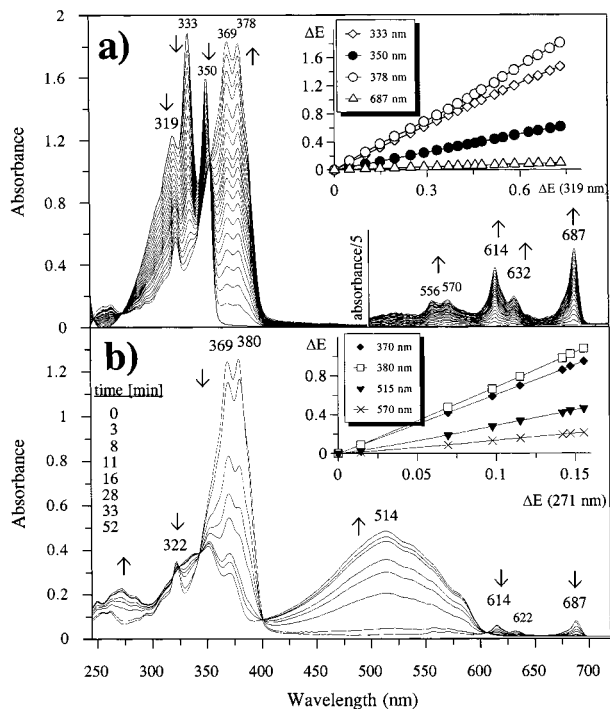
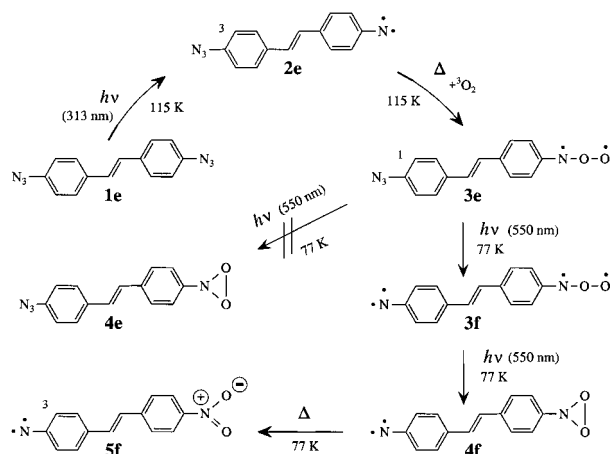


**Figure 2.** UV/vis spectroscopic investigations of **1a** → **3a** in MTHF: (a) low-light intensity photolysis ( $\lambda_{\text{exc}} = 313$  nm) of 4-azidostilbene (**1a**,  $\lambda_{\text{max}} = 319, 333,$  and  $350$  nm) and an ED diagram and (b) thermal reaction of 4-nitrene-substituted stilbene (**2a**,  $\lambda_{\text{max}} = 369, 378, 614,$  and  $687$  nm) in forming the nitroso oxide **3a** ( $\lambda_{\text{max}} = 514$  nm) and an ED diagram.

### Scheme 3



thermally stable at 77 K. This was also observed in the case of **2b–d**.

The UV/vis spectra obtained after the thermal reaction of the triplet nitrene **2a** in air-saturated MTHF at 95 K are shown in Figure 2b. From this, it follows that **2a** reacts quantitatively to form species **3a** ( $\lambda_{\text{max}} = 514$  nm). The 4-aminostilbene ( $\lambda_{\text{max}} = 351$  nm) is not formed here at 95 K.<sup>8</sup> The linear ED curves in the inset of Figure 2b indicate that **3a** is formed from **2a** in only one observable reaction step.

(8) The triplet nitrenes that were used are photochemically stable. Since MTHF is totally rigid at 77 K, significant bimolecular thermal reactions can also be excluded. Between 77 and 100 K, two bimolecular thermal reactions occur. These are the hydrogen abstraction from the matrix solvent and the reaction of the triplet nitrene with molecular oxygen. The yields of these reactions are significantly influenced by the matrix viscosity and therefore by the temperature. Below 86 K, the triplet nitrenes prefer to react under hydrogen abstraction to form the corresponding primary amines. Above 92 K, the MTHF matrix is soft, which only leads to the formation of the corresponding nitroso oxides **3a–d**.<sup>5,7,16</sup>

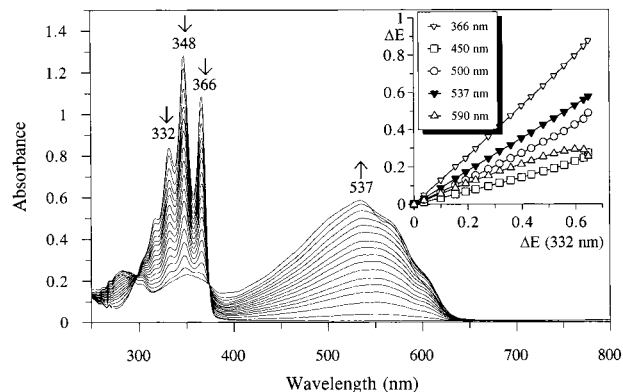


**Figure 3.** UV/vis spectra of the "low light intensity photolysis" ( $\lambda_{\text{exc}} = 313$  nm) of 4,4'-diazidostilbene (**1e**,  $\lambda_{\text{max}} = 332, 348,$  and  $366$  nm) at 115 K in MTHF and formation of the nitroso oxide **3e** ( $\lambda_{\text{max}} = 537$  nm).

On the basis of the subsequent photochemical and thermal reactions of **3a** (including product analysis)<sup>9</sup> and considering the spectroscopic results of Brinen et al.,<sup>4</sup> it is concluded that **3a** is the nitroso oxide. Our parallel ESR spectroscopic investigations showed that no signal exists for **3a** at 77 K. This indicates that the observed subsequent reactions should start from the singlet state of **3a**.<sup>10</sup>

As mentioned above, the triplet nitrenes **2b–d** were generated in the same way and the nitroso oxides **3b–d** were formed under conditions similar to those of **3a** ( $T = 95$  K, in MTHF). The nitroso oxide **3e** was formed in a different way (Scheme 3). First, 4,4'-diazidostilbene (**1e**) was photolyzed using low light intensities<sup>11</sup> ( $\lambda_{\text{exc}} = 313$  nm) at 115 K in MTHF. Under these conditions, the primarily formed triplet azidonitrene **2e** reacts immediately with dissolved triplet oxygen to form species **3e** ( $\lambda_{\text{max}} = 537$  nm, Figure 3).

The UV/vis spectra of all nitroso oxides (**3a–e**) are shown in Figures 4 and 5 (broken lines), the spectroscopic properties of all involved species are summarized in Table 1.

After photolysis of the nitroso oxides **3a–e**, different intermediates are observed using stationary UV/vis spectroscopy. The kind of observed intermediates strongly depends on light intensity and temperature. If the nitroso oxides **3a–e** are excited monochromatically ( $\lambda_{\text{exc}} = 550$  nm for **3a** and **3e**,  $\lambda_{\text{exc}} = 480$  nm for **3b**,  $\lambda_{\text{exc}} = 675$  nm for **3c**, and  $\lambda_{\text{exc}} = 625$  nm for **3d**) at 95 K using a low light intensity,<sup>11</sup> then only the nitro products **5a–d** and **5f** are observed in the UV/vis spectrum. As an example, this is shown in Figure 4a for the stepwise low-intensity irradiation of **3b** ( $\lambda_{\text{max}} = 483$  nm for **3b**, and  $\lambda_{\text{max}} = 357, 374,$  and  $394$  nm for **5b**).<sup>13</sup> While the ED curves of the stepwise low-intensity photolyses of **3a–e** are linear at 95 K, the ED curves of the same reactions at 77 K are generally nonlinear. If additionally strong light intensities<sup>11</sup> are used (at

(9) Species **3a–d** are not formed in anaerobic MTHF. After excitation of **3a–d** between 77 and 100 K, the corresponding nitro compounds are the final products. The thermal reaction of **3a–d** ( $T > 120$  K) leads finally to the formation of the nitroso compounds. The UV/vis spectra of nitroso compounds are always red-shifted compared with those of the corresponding nitro compounds [e.g., for 4-nitrostilbene,  $\lambda_{\text{max}} = 354$  nm; for 4-nitrosostilbene,  $\lambda_{\text{max}} = 386$  nm (in methanol at 25 °C)].

(10) The species **3a–e** have similar UV/vis spectroscopic properties. Furthermore, they show the same consecutive photochemical and thermal reactions. It is therefore assumed that at 77 K **3b–e** also exist in their singlet states. Their electronic states below 77 K were not investigated in this work.

(11) The experimental conditions for the "low light intensity" and for the "strong light intensity" photolyses are described in the Experimental Section.

(12) The  $\lambda_{\text{fs}}$  for **2f** is similar to the value observed by: Minato, M.; Lathi, P. M. *J. Am. Chem. Soc.* **1997**, *119*, 2187.

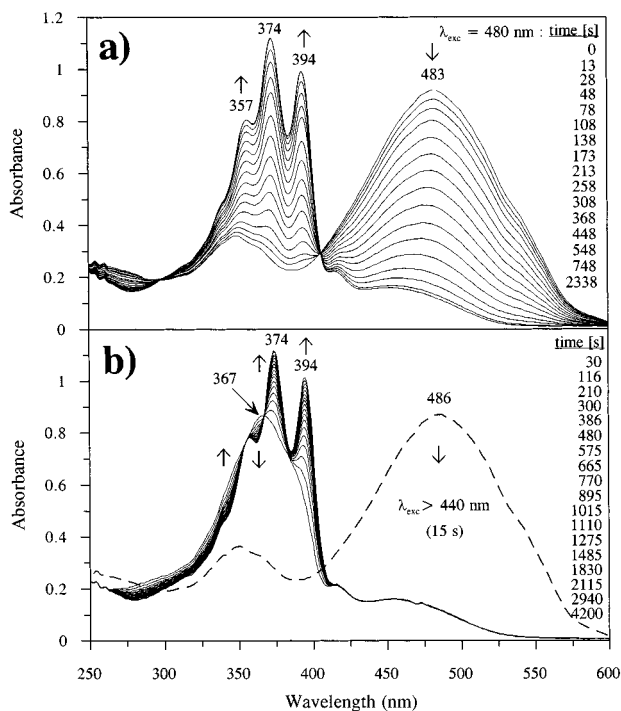


**Figure 4.** UV/vis spectroscopic investigations of **3b**  $\rightarrow$  **5b** in MTHF: (a) “low light intensity photolysis” ( $\lambda_{\text{exc}} = 480$  nm, irradiation time is given in the picture) of the nitroso oxide **3b** ( $\lambda_{\text{max}} = 483$  nm) at 95 K and formation of 4,4'-dinitrostilbene (**5b**,  $\lambda_{\text{max}} = 357, 374,$  and  $394$  nm) without observable intermediates; and (b) “strong light intensity photolysis” ( $\lambda_{\text{exc}} > 440$  nm) of the nitroso oxide **3b** ( $\lambda_{\text{max}} = 486$  nm) at 77 K, formation of the dioxaziridine **4b** ( $\lambda_{\text{max}} = 367$  nm), and its thermal reaction (the time is given in the picture) in forming 4,4'-dinitrostilbene (**5b**,  $\lambda_{\text{max}} = 357, 374,$  and  $394$  nm).

77 K), then the absorption bands of unstable intermediates (**4a–d** and **4f**) are observed. At 77 K, these intermediates (**4a–d** and **4f**) react thermally to form the corresponding nitro compounds. As an example, this is demonstrated in Figure 4b for the photochemically induced reaction of **3b** ( $\lambda_{\text{max}} = 486$  nm), which forms **4b** ( $\lambda_{\text{max}} = 367$  nm), and for the subsequent thermal reaction of **4b**, which forms **5b** ( $\lambda_{\text{max}} = 374$  and  $394$  nm). This means that a high stationary concentration of **4b** is obtained using strong light intensities at 77 K (Figure 4b) but not if low light intensities are used at 95 K (Figure 4a). If **3b** is excited using strong light intensities at 95 K, then only a small concentration of **4b** is obtained. This indicates that the primary photochemical reaction after excitation of **3b** is the same at both temperatures, but a sufficient stabilization of **4b** is only possible at 77 K.

The irradiation of **3a**, **3c**, **3d**, and **3e** leads qualitatively to the same reactions; all important experimental results are shown in Figure 5a–d (for the assignment of the intermediates, compare to Table 1). The photolysis of **3e** at 77 K ( $\lambda_{\text{exc}} = 550$  nm) leads additionally to the loss of nitrogen and to the formation of **3f** ( $\lambda_{\text{max}} = 554$  nm).<sup>14</sup> Species **3f** cannot be stabilized since it is also photolyzed under the given conditions,

(13) The nitro products **5a–d** were identified by their UV/vis spectra at 77 K by comparing them with spectra of authentic samples (at 77 K) as well as by product analysis (HPLC using reference substances) at 300 K. Species **5f** (UV/vis:  $\lambda_{\text{max}} = 379, 396, 454$  nm; ESR:  $H_{\text{xy}} = 620.7$  mT,  $|D/hc| = 0.8$  cm<sup>-1</sup>) was identified by comparing its UV/vis and ESR spectra with those of 4-nitrene-substituted 4'-nitrostilbene which was generated independently by the photolysis of 4-azido-4'-nitrostilbene (at 77 K).<sup>7</sup>

(14) Since the quantum yield of the nitrogen extrusion (**3e**  $\rightarrow$  **3f**) is much higher than that of the electrocyclization (**3e**  $\rightarrow$  **4e**), the observation of the azidodioxaziridine **4e** is impossible.

thus forming species **4f** ( $\lambda_{\text{max}} = 355$  and  $371$  nm, Figure 5a, Scheme 3).<sup>15</sup>

It follows from Figures 4b and 5a–d that the intermediates **4a–d** and **4f** are highly reactive at 77 K in the dark ( $\tau_{1/2} \approx 4$  min). As mentioned, their thermal reactions lead in all the cases that were investigated to the formation of the corresponding nitro compounds **5a–d** and **5f**. The ED curves of the thermal reactions of **4a–d** and **4f** in forming **5a–d** and **5f** at 77 K are strongly linear. This demonstrates that only one thermal process is observed. This process is very fast compared with thermal bimolecular processes in MTHF at 77 K.<sup>7,16</sup> It is therefore concluded that the reactions of **4a–d** and **4f** in forming **5a–d** and **5f** are intramolecular processes. Considering the exclusive formation of the nitro derivatives **5a–d** and **5f** and the inability of oxygen and other species to diffuse at this temperature, it is concluded from mechanistic arguments that the intermediates **4a–d** and **4f** are the corresponding dioxaziridines (Schemes 2 and 3). The proposed reactions of the nitroso oxides **3a–d** and **3f** are supported by the fact that similar 1,3-dipoles show similar intramolecular reactions. The photochemical disrotatory ring closure in forming three-membered heterocycles is allowed by orbital symmetry rules and well-known for other 1,3-dipoles such as carbonyl oxides or azomethine ylides. The conrotatory ring opening reaction proceeds thermally. The product is another isomeric 1,3-dipole.<sup>17</sup>

On the basis of the analogy of the reactions of 1,3-dipoles such as carbonyl oxides, another possible candidate for **4** might be the nitroso compound formed after excitation of the nitroso oxide. The nitroso compound would then react ultimately with oxygen to form the corresponding nitro compound. But this reaction way can be excluded because of our experimental data since it is well-known that UV/vis absorption bands of aromatic nitroso compounds are always strongly red shifted compared to those of the corresponding nitro compounds.<sup>9</sup> On the basis of the kinetic analyses of the reactions **3**  $\rightarrow$  **4**  $\rightarrow$  **5** (described above) and on the basis of mechanistic arguments, the intermediate **4** can also be excluded to be ArNHOO<sup>•</sup> or a dehydroazepine. Furthermore, **4** cannot be a product with the solvent (ArNH<sup>•</sup>) since its formation and the formation of the final nitro product depend on the presence of oxygen.<sup>9</sup>

When all these arguments are considered, it is almost certain that the intermediates **4a–d** and **4f** are the dioxaziridines.

The fast thermal reactions of **4a–d** and **4f** at 77 K indicate that the dioxaziridines are highly reactive species. The first-order rate constants ( $k$ ) of the ring opening reactions of **4a–d** and **4f** were obtained by monitoring the absorbance ( $E$ ) as a function of time. The  $k$  values (at 77 K) were calculated from the slopes of these plots. They are, within experimental error, all equal to  $0.0030 (\pm 0.0005) \text{ s}^{-1}$ . This means that the reaction is not influenced by mesomerically (**4a**) and inductively (**4b**) electron-withdrawing or mesomerically electron-donating (**4d**) substituents at the 4'-position of the stilbene or biphenyl.

**Ab Initio Calculations.** It was the aim of our ab initio calculations to find a confirmation of our experimental findings described above. We have chosen the nonsubstituted dioxaziri-

(15) The absorption bands at 541 and 573 nm are caused by the di-nitroso oxide) which is formed in a side reaction during the photolysis of **1e** at 115 K in MTHF.<sup>5</sup> This intermediate is photochemically stable and can be formed either by a strong light intensity photolysis of **1e** at 115 K in MTHF or by the thermal reaction of **2f** (generated before at 77 K) at  $T > 95$  K.

(16) Harder, T.; Stösser, R.; Wessig, P.; Bendig, J. *J. Photochem. Photobiol., A* **1997**, *103*, 105.

(17) Scaiano, J. C. In *Handbook of Organic Photochemistry*; CRC Press: Boca Raton, FL, 1989.

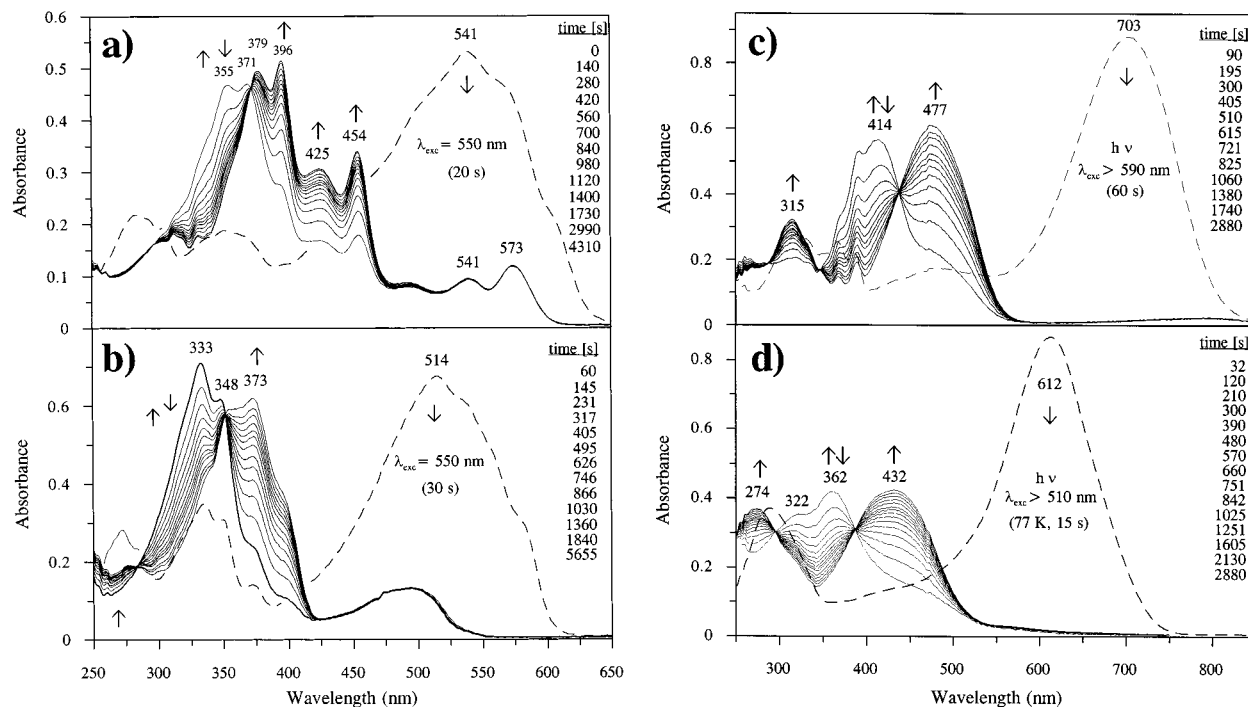


**Figure 5.** UV/vis spectroscopic investigations of the “strong light intensity photolyses” of the nitroso oxides and of the thermal reactions of dioxaziridines at 77 K (the time of the thermal reaction  $4 \rightarrow 5$  is given in each figure): (a) photolysis ( $\lambda_{\text{exc}} = 550 \text{ nm}$ ) of the nitroso oxide **3e** ( $\lambda_{\text{max}} = 541 \text{ nm}$ ), formation of the dioxaziridine **4f** ( $\lambda_{\text{max}} = 355$  and  $371 \text{ nm}$ ), and its thermal reaction in forming the 4-nitrene-substituted 4'-nitrostilbene (**5f**,  $\lambda_{\text{max}} = 379, 396, 425,$  and  $454 \text{ nm}$ );<sup>15</sup> (b) photolysis ( $\lambda_{\text{exc}} = 550 \text{ nm}$ ) of the nitroso oxide **3a** ( $\lambda_{\text{max}} = 514 \text{ nm}$ , compare to Figure 2b), formation of the dioxaziridine **4a** ( $\lambda_{\text{max}} = 333$  and  $348 \text{ nm}$ ), and its thermal reaction in forming 4-nitrostilbene (**5a**,  $\lambda_{\text{max}} = 373 \text{ nm}$ ); (c) photolysis ( $\lambda_{\text{exc}} > 590 \text{ nm}$ ) of the nitroso oxide **3c** ( $\lambda_{\text{max}} = 703 \text{ nm}$ ), formation of the dioxaziridine **4c** ( $\lambda_{\text{max}} = 414 \text{ nm}$ ), and its thermal reaction in forming 4-(dimethylamino)-4'-nitrostilbene (**5c**,  $\lambda_{\text{max}} = 477 \text{ nm}$ ); and (d) photolysis ( $\lambda_{\text{exc}} > 510 \text{ nm}$ ) of the nitroso oxide **3d** ( $\lambda_{\text{max}} = 612 \text{ nm}$ ), formation of the dioxaziridine **4d** ( $\lambda_{\text{max}} = 362 \text{ nm}$ ), and its thermal reaction in forming 4-amino-4'-nitrobiphenyl (**5d**,  $\lambda_{\text{max}} = 432 \text{ nm}$ ).

**Table 1.** UV/Vis and ESR Spectroscopic Properties of the Compounds Investigated at 77 K in MTHF

substituent derivative	$R = -N_3$ <b>1</b>	$R = \cdot\dot{N}$ <b>2</b>	$R = \cdot\dot{N}-O-\dot{O}$ <b>3</b>	$R = \cdot\dot{N}-O-\dot{O}$ <b>4</b>	$R = \cdot\dot{N}-O-\dot{O}$ <b>5</b>
	$\lambda_{\text{max}} [\text{nm}]$	$ D/hc  [\text{cm}^{-1}]$ $\lambda_{\text{max}} [\text{nm}]$	$\lambda_{\text{max}} [\text{nm}]$	$\lambda_{\text{max}} [\text{nm}]$	$\lambda_{\text{max}} [\text{nm}]$
	319, 333, 350	0.800 369, 378 614, 687	514	333, 348	373
	288, 389	0.801 380, 395 419, 450	486	367	357, 374, 394
	375, 394	0.750 479 674, 750	703	414	477
	322	0.860 388, 607	612	362	432
	334, 350, 369	0.796 403 640, 717	541	—	389
	403, 640, 717	0.122 <sup>12</sup> (quinonoid)	405, 434	554	355, 371 379, 396 425, 454

dine **6** and *N*-phenyldioxaziridine **9** as model systems for the calculations. All calculations were performed with the program GAUSSIAN 94.<sup>18</sup>

First, we have investigated the structures of the dioxaziridines **6** and **9** using the well-established hybrid DFT method Becke3Lyp<sup>19</sup> and the 6-31G\* basis set.<sup>20</sup> Figure 6 shows the

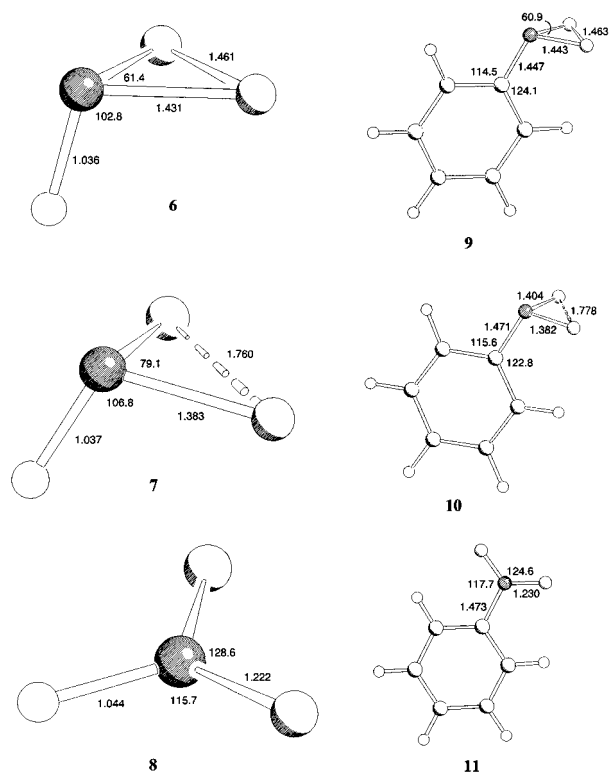


**Figure 6.** Calculated structures of the dioxaziridines **6** and **9**, the nitro derivatives **8** and **11** formed by ring opening, and the corresponding transition states **7** and **10**.

optimized structures and the most important geometrical parameters of the calculated species. One can see that the structures of both dioxaziridines are very similar concerning the three-membered ring. The nitrogen atom is strongly pyramidalized even though the reason is not a  $sp^3$  hybridization but a cyclopropane-like electronic structure of the ring. This is confirmed by the structure of *N*-phenyldioxaziridine **9**. The phenyl substituent prefers a bisected conformation, which points to an overlap of  $\pi$  orbitals of the aromatic ring and a Walsh orbital of the nitrogen atom, a phenomenon well-known from substituted cyclopropanes.<sup>21</sup> It should be noted that the perpendicular conformation of **9** was found to be a transition state. The rotation barrier amounts to 3.5 kcal/mol (B3Lyp/6-31G\*).

Second, we were interested in the transition state of the ring opening in forming isonitrous acid **8** and nitrobenzene **11**. Kahn et al.<sup>22</sup> recently concluded that the isonitrous acid **8** has a remarkably diradical character. This was concluded by the fact that a spin-unrestricted Hartree–Fock (UHF) wave function provides a lower energy than a spin-restricted Hartree–Fock (RHF) treatment. Therefore, an investigation of the reaction path

(18) Frisch, M. J.; Trucks, G. W.; Schlegel, H. B.; Gill, P. M.; Johnson, B. G.; Robb, M. A.; Cheeseman, J. R.; Keith, T.; Petersson, G. A.; Montgomery, J. A.; Raghavachari, K.; Al-Laham, M. A.; Zakrzewski, V. G.; Ortiz, J. V.; Foresman, J. B.; Cioslowski, J.; Stefanov, B. B.; Nanayakkara, A.; Challacombe, M.; Peng, C. Y.; Ayala, P. Y.; Chen, W.; Wong, M. W.; Andres, J. L.; Replogle, E. S.; Gomperts, R.; Martin, R. L.; Fox, D. J.; Binkley, J. S.; Defrees, D. J.; Baker, J.; Stewart, J. P.; Head-Gordon, M.; Gonzalez, C.; Pople, J. A. *Gaussian 94*; Gaussian, Inc.: Pittsburgh, PA, 1995.

(19) Parr, R. G.; Yang, W. *Density-Functional Theory of Atom and Molecules*; Oxford University Press: New York, 1989.

(20) Hariharan, P. C.; Pople, J. A. *Chem. Phys. Lett.* **1972**, *66*, 217.

(21) Hehre, W. J.; Rado, L.; Schleyer, P. v.; Pople, J. A. *Ab initio Molecular Orbital Theory*; John-Wiley & Sons: New York, 1986.

(22) Kahn, S. D.; Hehre, W. J.; Pople, J. A. *J. Am. Chem. Soc.* **1987**, *109*, 1871.

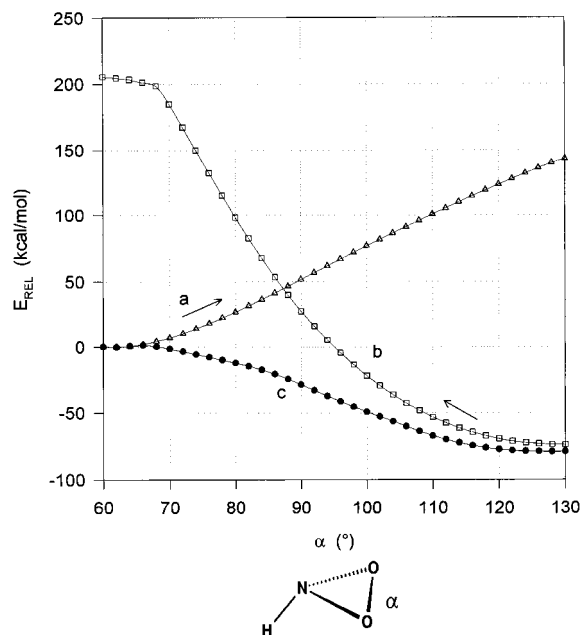


**Figure 7.** Energy of HNO<sub>2</sub> upon variation of bond angle ( $\alpha$ ) O–N–O (HF/6-31G\*): (a) electronic state of **6** kept along the reaction path, (b) electronic state of **8** kept along the reaction path, and (c) new guess at every point of the reaction path.

**6**  $\rightarrow$  **8** should also demand a spin-unrestricted treatment. Figure 7 shows the results of reaction path calculations upon variation of the bond angle O–N–O ( $\alpha$ ). It was surprising that starting with the geometry of **6** increasing values of  $\alpha$  provided a continuous increase of energy (Figure 7, curve a). The same result was obtained in the reverse direction starting with the geometry of **8** (curve b). Obviously, a far-reaching change of the MO scheme takes place along the reaction path. The steady energy (curve c) was first obtained by a new guess of the UHF wave function at every point and second by mixing the HOMO and LUMO in the wave function to destroy  $\alpha$ - $\beta$  and spatial symmetries (this is often necessary if a stable UHF wave function of a singlet state with diradical character is produced).

Since the electron correlation is neglected in this method and due to the well-known tendency of UHF wave functions to be spin-contaminated, the Hartree–Fock values shown in Figure 7 should not be overestimated. Nevertheless, these results encouraged us to investigate the stereoelectronic course of the reaction by means of Hartree–Fock theory. Figure 8 shows the orbital correlation diagram obtained on the HF/6-31G\* level. The five highest occupied molecular orbitals and the lowest unoccupied molecular orbital of both **6** (left) and **8** (right) are shown. It is easy to recognize that the LUMO of **6**, an antibonding Walsh orbital, corresponds with HOMO-2 of **8**, a nonbonding n orbital. On the other hand, the HOMO of **6**, an n orbital with a weak O–O  $\pi$  interaction, corresponds with the LUMO of **8**, an antibonding  $\pi^*$  orbital.

One can therefore deduce from the orbital correlation diagram which reactant and product configurations correlate with each other. The diagram shown in Figure 8 suggests that correlation lines of equal symmetry cross in a configuration diagram. This is a violation of the noncrossing rule, and therefore, **6**  $\rightarrow$  **8** must be considered as a symmetrical ground state-forbidden concerted reaction path.

Nevertheless, the reaction was found to be strongly exothermic, which means that a little activation barrier is expected. To obtain more accurate activation barriers, the ring openings of **6**

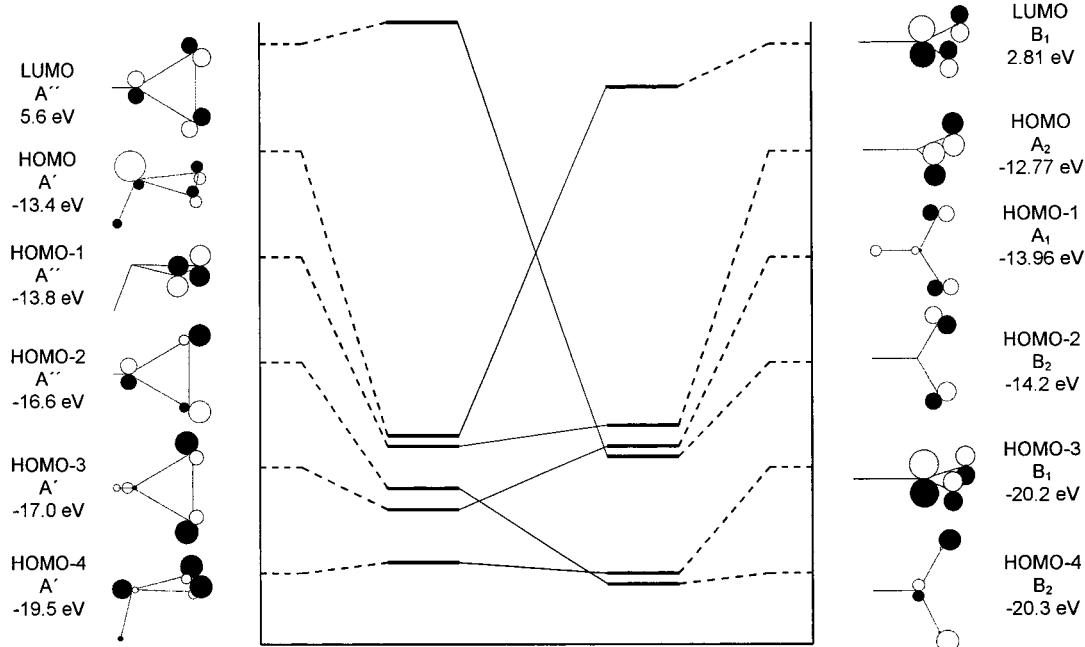


**Figure 8.** Orbital correlation diagram for the reaction path **6** → **8** (HF/6-31G\*).

**Table 2.** Calculated Energies of **6–11** (UB3Lyp/6-31G\*\*/UB3Lyp/6-31G\*)

entry	<i>E</i> (au)	ZPVE (kcal/mol)	$\Delta E^a$ (kcal/mol)
<b>6</b>	-205.5670	12.6	0
<b>7</b>	-205.5411	10.5	14.2
<b>8</b>	-205.6869	13.8	-74.0
<b>9</b>	-436.6261	63.2	0
<b>10</b>	-436.5867	61.6	18.8
<b>11</b>	-436.7506	65.0	-80.7

<sup>a</sup> Relative energies including zero-point energy,  $\Delta E = E - E(\mathbf{6})$  and  $\Delta E = E - E(\mathbf{9})$ , respectively.

and **9** were reinvestigated using a wave function which includes electron correlation (B3Lyp/6-31G\*). The resulting structures of the transition states **7** and **10** are pictured in Figure 6. We have found energy differences of 14.2 kcal/mol (**6** → **7**) and 18.8 kcal/mol (**9** → **10**). All thermodynamic parameters of the model compounds **6–11** are shown in Table 2.

Unfortunately, it is not possible to compare our calculated energy barriers with the experimental data because different molecules were investigated experimentally and theoretically. As mentioned in the Introduction, this was inevitable because of two reasons. On one hand, large molecules are the precondition for an experimental success (photochemically stable triplet nitrenes must be generated and different species must be able to be distinguished by UV/vis spectroscopy), but on the other hand, only small molecules can be treated quantum chemically at a high level of theory. Furthermore, it is generally impossible to estimate a reliable energy barrier on the basis of only one rate constant determined experimentally at one temperature (especially if the reaction was carried out in a low temperature matrix). Energy barriers can therefore not be compared quantitatively. But it can be concluded from the theoretical results that dioxaziridines are separated from their appropriate nitro products by an orbital symmetry-forbidden barrier and that they are experimentally observable species.

## Conclusions

Aromatic nitroso oxides can be synthesized quantitatively by a thermal reaction of the corresponding triplet nitrenes in air-

saturated MTHF at 95 K. At temperatures below 100 K, aromatic nitroso oxides are thermally stable. The investigated nitroso oxides **3a–e** exist at 77 K in their singlet states. Hitherto assumed but not found, further intermediates were directly observed by UV/vis spectroscopy after optical excitation of nitroso oxides at 77 K. On the basis of their UV/vis spectra and chemical, mechanistic, and kinetic arguments, these intermediates are assumed to be the corresponding dioxaziridines, but more analytical results (IR spectra) are necessary to prove this statement. The assumed dioxaziridines **4a–d** and **4f** are highly reactive species. They react thermally ( $k_{77\text{K}} = 0.003 \text{ s}^{-1}$ ) to form the corresponding nitro compounds (**5a–d** and **5f**). The velocity of the ring opening reaction is mainly determined by the strained dioxaziridine structure but not by substituents.

It follows from ab initio calculations that dioxaziridines are experimentally observable species. They are separated from the nitro products by an orbital symmetry-forbidden barrier.

## Experimental Section

**General.** The starting reagents were used as purchased from Aldrich Chemical Co. MTHF (2-methyltetrahydrofuran) was distilled from calcium hydride. Optical absorption measurements were carried out with a Hitachi U-3410 double-beam spectrophotometer using a 1 mm quartz cell. The temperature could be adjusted and kept constant between 77 and 300 K with a precision of 0.1 K using a cryostat equipped with a temperature controller. The ESR spectra were recorded on a ERS 300 spectrometer (ZWG Berlin, X-band microwave unit, 100 kHz field modulation,  $f = 9.18 \text{ GHz}$ ). The samples were cooled within the cavity using a liquid nitrogen Dewar insert. The product analysis was realized by HPLC investigations (Kontron, DAD 440) comparing both the retention time and the UV/vis spectra of the products with those of reference substances.

**Irradiation.** For both the UV/vis and ESR experiments, the light sensitive compounds were irradiated through a water cell (10 cm), metal interference filters, and/or glass filters using a high-pressure mercury lamp (500 W) at a distance of 20 cm. The samples were irradiated within the sample chambers of the spectrometers.

The so-called "low light intensity photolysis" was realized by the combination of both a metal interference filter (for  $\lambda_{\text{exc}}$  see the text)

and glass filters which decreased the light intensity additionally. The light intensity was adjusted according to the following criteria. In the starting period of the photolysis, 5 s of irradiation must decrease  $E$  by about 0.05 [ $E_0$  ( $\lambda_{\text{max}}$ )  $\approx$  1]. It was irradiated in intervals of about 5 s, and after every irradiation, the sample was in the dark for at least 3 min. The spectra were recorded during this time. This kind of irradiation was applied to the photolysis of all nitroso oxides and azides [ $\lambda_{\text{exc}}$ (**1a**, **1d**, **1e**) = 313 nm,  $\lambda_{\text{exc}}$ (**1b**, **1c**) = 365 nm]. UV/vis spectra obtained by this procedure are shown in Figure 2a (photolysis of **1a**, formation of **2a**), in Figure 3 (photolysis of **1e**, formation of **3e**), and in Figure 4a (photolysis of **3b**, formation of **5b**).

The so-called "strong light intensity photolysis" was realized by using either only metal interference filters or only glass filters. The light intensity was adjusted here according to the following criteria. The light sensitive intermediate must be completely decomposed after a single irradiation process which must not exceed 30 s. After this single photolysis, the UV/vis spectra were quickly recorded using the highest speed of the spectrophotometer (1200 nm/min). Species **3a** and **3e** ( $\lambda_{\text{exc}}$  = 550 nm) were irradiated using only a metal interference filter, and species **3b** ( $\lambda_{\text{exc}}$  > 440 nm), **3c** ( $\lambda_{\text{exc}}$  > 590 nm), and **3d** ( $\lambda_{\text{exc}}$  > 510 nm) were irradiated using only a glass filter. Reference experiments showed that qualitatively the same reactions occur when the intermediates **3b–d** are irradiated using metal interference filters. UV/vis spectra obtained by this procedure are shown in Figure 4b (photolysis of **3b**, formation of **4b**) and Figure 5 (photolysis of **3a**, **3c**, **3d**, and **3e**).

**trans-4-Nitrostilbene.** Benzaldehyde (9.2 g), 1.5 mL of freshly distilled piperidine, and 16 g of (nitrophenyl)acetic acid were combined and refluxed for 2 h in an oil bath at 140 °C. After cooling to room temperature, the yellow residue was treated with ethanol. It was filtered and recrystallized from ethanol (85% yield). Anal. Calcd: C, 74.65; H, 4.9; N, 6.2. Found: C, 74.4; H, 4.7; N, 6.0. UV/vis:  $\lambda_{\text{max}}$  = 354 nm (methanol). Mp: 155 °C.

**trans-4-Aminostilbene.** *trans-4'*-Nitrostilbene (3.5 g) was suspended in 100 mL of 80% ethanol. Then a solution of 35 g of  $\text{FeSO}_4 \cdot 7\text{H}_2\text{O}$  in 175 mL of water treated with 175 mL of concentrated  $\text{NH}_3$  was added. Subsequently, the reaction mixture was heated on a steam bath for 2 h and cooled to room temperature. After 12 h, the mixture was filtered and the black residue was extracted several times using diethyl ether. After evaporation of the solvent, the product was recrystallized from ethanol to provide a yield of 90%. Anal. Calcd: C, 86.1; H, 6.7; N, 7.1. Found: C, 85.7; H, 6.6; N, 6.7. UV/vis:  $\lambda_{\text{max}}$  = 324 nm (methanol).

**trans-4-Azidostilbene (1a).** Concentrated HCl (20 mL) and 20 mL of water were added to 3.7 g of *trans-4*-aminostilbene. The mixture was cooled to  $-10$  °C and treated dropwise (0.5 h) with a solution of 0.67 g of  $\text{NaNO}_2$  in 5 mL of water, and then stirred for another 1.5 h at  $-10$  °C. The reaction mixture was filtered at 0 °C. A solution of 0.7 g of  $\text{NaN}_3$  in 10 mL of water was added (0.5 h). The solution was stirred for another 1.5 h at 0 °C. The solid was filtered, rinsed with water, and dried (85% yield). Anal. Calcd: C, 75.99; H, 5.01; N, 18.99. Found: C, 75.03; H, 5.06; N, 18.71. UV/Vis:  $\lambda_{\text{max}}$  = 324 nm (methanol). IR (KBr): 2121.3  $\text{cm}^{-1}$  (str N=N=N). Mp: 104 °C.

**trans-4,4'-Dinitrostilbene.**<sup>23</sup> 4-Nitrobenzyl chloride (10 g) was dissolved in 30 mL of heated ethanol. Then 3.5 g of KOH, dissolved in a mixture of 3 mL of water and 12 mL of ethanol, was added dropwise at 25 °C. The temperature of the reaction mixture was raised to about 70 °C. It was stirred for 2 h at 70 °C, cooled, and filtered. The residue was washed with ethanol. The crystals were yellow needles (80% yield). Anal. Calcd: C, 62.2; H, 3.7; N, 10.4. Found: C, 62.1; H, 3.7; N, 10.1. UV/Vis:  $\lambda_{\text{max}}$  = 353 nm (methanol). Mp: 282 °C.

**trans-4-Amino-4'-nitrostilbene.**<sup>24</sup> *trans-4,4'*-Dinitrostilbene (5 g) was suspended in 200 mL of 95% ethanol. The mixture was stirred and heated to boiling. Then 13 mL of a 1.25 M solution of sodium sulfide, treated with hydrogen sulfide for 25 min, was added. After the

solution had turned dark red, it was evaporated to dryness. The residue was extracted with acetone and recrystallized from acetone. The crystals were red (52% yield). Anal. Calcd: C, 70.0; H, 5.0; N, 11.7; O, 13.3. Found: C, 69.3; H, 5.0; N, 11.5. UV/Vis:  $\lambda_{\text{max}}$  = 287, 403 nm (methanol). Mp: 201 °C.

**trans-4-Azido-4'-nitrostilbene (1b).** Concentrated HCl (20 mL) was added to 1.56 g of *trans-4*-amino-4'-nitrostilbene. The mixture was cooled to  $-10$  °C and treated dropwise (1.5 h) with a solution of 0.46 g of  $\text{NaNO}_2$  in 5 mL of water and then stirred for another 6 h at  $-10$  °C. Then the reaction mixture was filtered at 0 °C. A solution of 0.46 g of  $\text{NaN}_3$  in 10 mL of water was added, and the solution was stirred for another 2 h at 0 °C. The solid was filtered, rinsed with water and then with diethyl ether, and dried (70% yield). Anal. Calcd: C, 63.2; H, 3.8; N, 21.0. Found: C, 62.2; H, 3.8; N, 20.6. UV/Vis:  $\lambda_{\text{max}}$  = 283, 364 nm (methanol). IR (KBr): 2114.4  $\text{cm}^{-1}$  (str N=N=N).

**trans-4-(Dimethylamino)-4'-nitrostilbene.** 4-(Dimethylamino)benzaldehyde (13.2 g), 1.5 mL of freshly distilled piperidine, and 16 g of (nitrophenyl)acetic acid were combined and refluxed for 2 h in an oil bath at 140 °C. After cooling to room temperature, the red solid was treated with ethanol, filtered, and recrystallized from ethanol (85% yield). Anal. Calcd: C, 71.6; H, 6.0; N, 10.4; O, 11.9. Found: C, 71.7; H, 6.1; N, 10.4. UV/vis:  $\lambda_{\text{max}}$  = 297, 425 nm (methanol). Mp: 257 °C.

**trans-4-Amino-4'-(dimethylamino)stilbene.** *trans-4*-(Dimethylamino)-4'-nitrostilbene (4.2 g) was suspended in 100 mL of 80% ethanol. Then a solution of 35 g of  $\text{FeSO}_4 \cdot 7\text{H}_2\text{O}$  in 175 mL of water treated with 175 mL of concentrated  $\text{NH}_3$  was added. Subsequently, the reaction mixture was heated on a steam bath for 2 h and then cooled to room temperature. After 12 h, the mixture was filtered and the black residue was extracted several times using diethyl ether to isolate the product. After evaporation of the solvent, the product was recrystallized from ethanol to provide a yield of 68%. Anal. Calcd: C, 80.6; H, 7.6; N, 11.8. Found: C, 76.9; H, 8.0; N, 11.2. UV/vis:  $\lambda_{\text{max}}$  = 353 nm (methanol). Mp: 179 °C.

**trans-4-Azido-4'-(dimethylamino)stilbene (1c).** Concentrated HCl (20 mL) was added to 1.5 g of *trans-4*-amino-4'-(dimethylamino)stilbene. The mixture was cooled in the dark to  $-10$  °C, treated dropwise (1.5 h) with a solution of 0.48 g of  $\text{NaNO}_2$  in 1 mL of water, and then stirred for another 5 h at  $-10$  °C. Then the reaction mixture was filtered in the dark at 0 °C. A solution of 0.45 g of  $\text{NaN}_3$  in 10 mL of water was added, and the solution was stirred for another 2 h at 0 °C (dark). The solid was filtered, rinsed with water, and dried (10% yield). Anal. Calcd: C, 72.7; H, 6.1; N, 21.2. Found: C, 71.9; H, 5.9; N, 20.8. UV/vis:  $\lambda_{\text{max}}$  = 358 nm (methanol). IR (KBr): 2113.7  $\text{cm}^{-1}$  (str N=N=N).

**4,4'-Diazidobiphenyl.** Concentrated HCl (20 mL) and 20 mL of water were added to 1.75 g of 4,4'-diaminobiphenyl. The mixture was cooled to  $-10$  °C, treated dropwise (0.5 h) with a solution of 0.67 g of  $\text{NaNO}_2$  in 5 mL of water, and then stirred for another 1.5 h at  $-10$  °C. The reaction mixture was filtered at 0 °C. A solution of 0.7 g of  $\text{NaN}_3$  in 10 mL of water was added (0.5 h). The solution was stirred for another 1.5 h at 0 °C. The solid was filtered, rinsed with water, and dried (80% yield). Anal. Calcd: C, 61.0; H, 3.4; N, 36.6. Found: C, 61.2; H, 3.5; N, 36.5. UV/Vis:  $\lambda_{\text{max}}$  = 294 nm (methanol). IR (KBr): 2134.0  $\text{cm}^{-1}$  (str N=N=N). Mp: 126 °C.

**4-Amino-4'-azidobiphenyl (1d).** 4,4'-Diazidobiphenyl (0.2 g) was suspended in 20 mL of 85% ethanol. The mixture was stirred and heated to boiling. Then 0.4 mL of a 1.25 M solution of sodium sulfide, treated for 25 min with hydrogen sulfide before, was added. After the solution had turned green, it was stirred at 70 °C for another 30 min. Then it was evaporated at room temperature. Besides the azidoamine, the residue contains the diamine, the diazide, and inorganic compounds. It was extracted and recrystallized from ethanol several times. After these procedures, the purity of **1d** was only about 90%. The final product was therefore purified by HPLC (11% yield). Anal. Calcd: C, 68.6; H, 4.8; N, 26.6. Found: C, 67.4; H, 4.1; N, 26.1. UV/Vis:  $\lambda_{\text{max}}$  = 298, 401 nm (methanol).

**trans-4,4'-Diazidostilbene (1e).** Concentrated HCl (20 mL) and 20 mL of water were added to 2 g of *trans-4,4'*-diaminostilbene. The mixture was cooled to  $-10$  °C, treated dropwise (0.5 h) with a solution of 0.67 g of  $\text{NaNO}_2$  in 5 mL of water, and then stirred for another 1.5

(23) Walden, P.; Kernbaum, A. *Ber.* **1890**, *23*, 1959. Oki, M.; Kunimoto, H. *Spectrochim. Acta* **1963**, *19*, 1463.

(24) Calvin, M.; Buckles *J. Am. Chem. Soc.* **1940**, *62*, 3324.



h at  $-10\text{ }^{\circ}\text{C}$ . The reaction mixture was filtered at  $0\text{ }^{\circ}\text{C}$ . A solution of 0.7 g of  $\text{NaN}_3$  in 10 mL of water was added (0.5 h). The solution was stirred for another 1.5 h at  $0\text{ }^{\circ}\text{C}$ . The solid was filtered, rinsed with water, and dried (75% yield). Anal. Calcd: C, 64.1; H, 3.8; N, 32.0. Found: C, 63.7; H, 3.9; N, 31.0. UV/Vis:  $\lambda_{\text{max}} = 340\text{ nm}$  (methanol). IR (KBr):  $2120.1\text{ cm}^{-1}$  (str N=N=N). Mp:  $162\text{ }^{\circ}\text{C}$ .

**Acknowledgment.** We thank the micro resist technology GmbH (Berlin), the Deutsche Forschungsgemeinschaft (Bonn), and the Fond der Chemischen Industrie (Frankfurt/Main) for financial support.

JA9803660